Available online at www.sciencedirect.com

SciVerse ScienceDirect

Ceramics International 39 (2013) 2575–2580

CERAMICS INTERNATIONAL

www.elsevier.com/locate/ceramint

Phase transformation of diamond-like carbon/silver composite films by sputtering deposition

Shyuan-Yow Chen[a,b,c], Keng-Liang Ou[d,e,f], Wei-Chen Huang[a,b], Kuo-Tien Chu[c,g,**], Shih-Fu Ou[d,e,f,h,*]

[a]*Department of Dentistry, Cathay General Hospital, Sijhih, Taipei 221, Taiwan*
[b]*Department of Dentistry, Cathy General Hospital, Taipei 106, Taiwan*
[c]*Department of Dentistry, College of Oral Medicine, Taipei Medical University*
[d]*Research Center for Biomedical Devices and Prototyping Production, Taipei Medical University, Taipei 110, Taiwan*
[e]*Research Center for Biomedical Implants and Microsurgery Devices, Taipei Medical University, Taipei 110, Taiwan*
[f]*Graduate Institute of Biomedical Materials and Tissue Engineering, Taipei Medical University, Taipei 110, Taiwan*
[g]*Division of ProsthodontDivision of Prosthodontics, Department of Dentistry, Taipei Medical University Hospital*
[h]*Institute of Mold & Die Engineering, National Kaohsiung University of Applied Sciences, Kaohsiung, 807, Taiwan*

Received 22 August 2012; received in revised form 5 September 2012; accepted 5 September 2012
Available online 24 September 2012

Abstract

This study fabricated hydrogenated diamond-like carbon/silver bioceramic films on glass substrates using radio frequency magnetron sputtering with a single silver target in an atmosphere of Ar/CH4 mixture. The effects of applied power on the composition and microstructure of bioceramic film were evaluated. A phase transformation, amorphous diamond-like carbon → nano-silver precipitation → nano-silver growth in the amorphous diamond-like carbon matrix was observed during sputtering. The film growth rate, surface roughness, silver content and size of silver nanoclusters in the films all increased with the silver target power due to the higher flux of sputtered silver species toward the substrate.

Keywords: B. Nanocomposites; Silver-containing diamond-like carbon; Sputtering

1. Introduction

Metastable amorphous carbon film exhibits a great variety of bonding structure and accordingly electrical, optical, chemical and mechanical properties [1,2]. By adjusting their microstructures and hybridizations, carbon films with various properties can be used in many applications, such as protective, heat-conducting, hydrophobic, biocompatible and other functional surface treatments on workpieces [3–6]. Most of the studies used low-temperature techniques to coat the amorphous hydrogenated carbon (a-C:H) films utilizing the plasma enhancement such as plasma enhanced chemical vapor deposition (PECVD) [7,8], ion beam deposition [9], magnetron sputtering [10,11], and vacuum arc deposition [12–15]. Generating plasma effectively decomposes and ionizes the hydrocarbon gas to synthesize a carbon film on substrate surface. Among these deposition techniques, magnetron sputtering and vacuum arc deposition are two mostly chosen processes because of their low cost, simplicity and competent deposition rate. However, the high residual stress accumulates with increasing film thickness, which causes the detachment of diamond-like carbon film from substrate [15–18]. It has been reported that the residual stress in diamond-like carbon (DLC) films can be reduced by doping metal elements or carbides [19–23]. Doping metal elements in a-C:H films do not only prevents the film detachment and improves the electric conductivity but also enables new antimicrobial functions to a-C:H films [23–25].

Many heavy metal elements have been found with antimicrobial ability [26]. Such antibacterial effect of metal

*Corresponding author. Graduate Institute of Biomedical Materials and Tissue Engineering, Taipei Medical University, Taipei 110, Taiwan.
**Corresponding author: Tel.: +886 227361661x5100; fax: +886 2 27395524.
E-mail address: m9203510@gmail.com

0272-8842/$ - see front matter © 2012 Elsevier Ltd and Techna Group S.r.l. All rights reserved.
http://dx.doi.org/10.1016/j.ceramint.2012.09.019

ions is long term and environment resistant, especially that of the silver nanoparticles. Not only their effectiveness against multiple drug-resistant bacteria by hindering respiration and division of bacteria, but also their limited toxicities to mammalian cells have been demonstrated [27,28]. It is generally reported that metal ions binding to thiol groups in enzymes and proteins play an essential role in antimicrobial action. In addition, metals deposited on cell membranes or cell walls can inhibit cell division and disrupt membrane integration [28,29].

The aim of the present work is to establish a reactive radio frequency (RF) magnetron sputtering process with single silver target to deposit silver-containing a-C:H films under an argon–methane mixture atmosphere. There are two ways to alter the contents of silver in the films: adjusting the mixture ratio of argon and methane at a constant target power, or adjusting the target power input under a constant argon–methane mixture atmosphere. Since adjusting the target power takes lesser process time and is more convenient for setting sequences in industrial processing, we chose the latter way in this study. The correlations between the target power and the structure of the synthesized films were investigated to evaluate the applicability of these films for potential usages.

2. Materials and methods

Glass substrates with a size of 1 cm in diameter and 2 mm in thickness were cleaned in an ultrasonic bath with the sequence of acetone followed ethanol for 15 min each. After air drying, the substrates were loaded into the deposition chamber. The reactive sputtering technique utilized in this study combines magnetron sputtering and RF plasma-enhanced chemical vapor deposition. The generated plasma species between sputtering gun and substrate simultaneously sputters the atoms of silver target material and decomposes the CH_4 gas as the carbon source for synthesizing the composite films. The setup of equipment and the detailed deposition procedures have been described in previous works [30,31]. The distance between silver target and substrates was fixed at 60 mm. After evacuating the chamber and heating the substrates to 200 °C, the methane–argon gas mixture in a ratio of 1/1.5 was introduced and the RF plasma was triggered. The deposition parameters are listed in Table 1.

The surface and cross-sectional morphologies of the deposited films were observed using a scanning electron microscope (SEM, JSM-6500) and an atomic force microscope (AFM, NanoMan NS4+D3100). The compositions of deposited films were analyzed using an energy dispersive X-ray spectrometer (EDX) attached on the scanning electron microscope. Since the hydrogen content in films cannot be analyzed by EDX, the ratio of measured Ag to C was used to represent the silver content in films. The crystallographic structures of films were characterized by grazing incidence X-ray diffraction (GIXRD, SIEMENS D5000), with a Cu Kα radiation source. A Raman spectrometer (BWTEK-MiniRam^{TM}II) was used to analyze the bonding of a-C:H phases in films. High-resolution transmission electron microscopy (HRTEM, PHILIPS F-20) was used to identify the structure of deposited film.

Table 1
Reactive sputtering deposition conditions for Ag/a-C:H films in this study.

Items	Parameters and values
Target material	Silver (purity 4 N, ψ7.62 cm)
Target power (W)	100, 150, 200, 250, 300
Substrate temperature (°C)	200
Gas flow ratio (Ar/CH_4)	1/1.5
Working pressure (Pa)	0.23
Deposition time (min)	25

3. Results and discussion

Fig. 1 shows the growth rate and Ag/C ratio of the films obtained at different target powers. With increase in the target power, the plasma density and accompanied ion bombardment on silver target intensify the flux of ejected silver species, which causes increased film growth rate and Ag/C ratio. The Ag/C ratio increases exponentially with target power, but the increase of film growth rate is not regular. Such nonlinear film growth rates induced by the target poisoning effect and electron–gas interactions of reactive gas molecules are commonly seen in an RF reactive sputtering process. For the films obtained at below 200 W target power, the fraction of silver in the films is minor, which indicates that the film growth rate at lower target power is mainly contributed by the deposition of the a-C:H matrix. The low fraction of silver can be attributed to the limited sputter yield of silver atoms with lower kinetic energy of incident ions and the formation of carbide on target surface (target poisoning). Large input energy is consumed by the complex interactions between hydrocarbon molecules and electrons, produceing various species which affect both the formation of carbide on silver target and films on formation. This causes irregularity of the film growth rate. Once the target power reaches 300 W, the emission rate and kinetic energy of ions are sufficient to remove the carbide on the target; the flux of silver suddenly increases and dominates the film growth rate.

The irregular dependence of intensity ratio, I_D/I_G, in Fig. 2 which was calculated from Raman spectra, also implies that these various bonds in films were caused by such complex plasma interactions. The I_D/I_G, an index of the disorder degree of a-C:H phase, initially decreases with the silver content, then rises to a maximum at 200 W, and subsequently decreases again. It disagrees with the typical trend of metal-doped a-C:H films that metal dopants promote the graphitization of carbon content [30]. However, other researches of Ag-incorporated a-C:H films using other deposition processes also indicated a similar irregularity at low silver content [32,33]. This irregularity could be

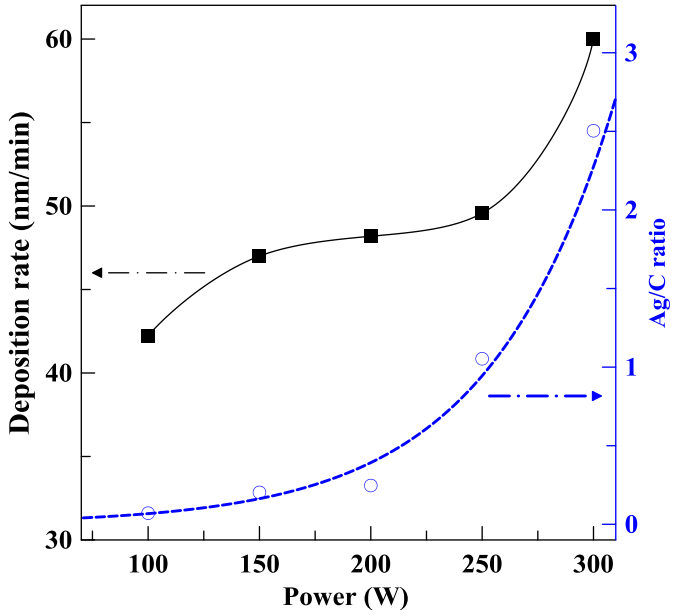

Fig. 1. Dependence of the film deposition rate and Ag/C ratio in film as a function of target power.

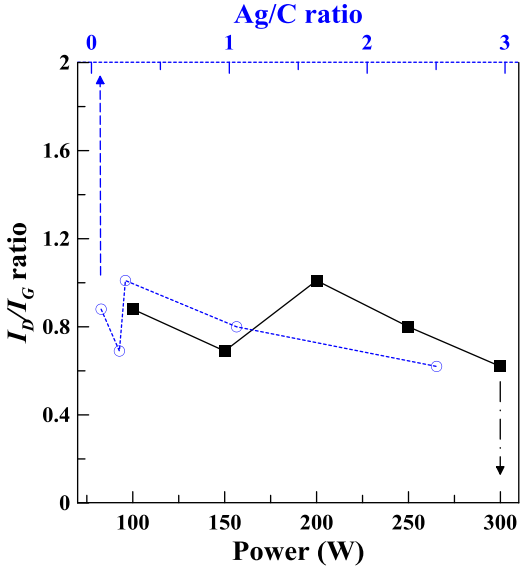

Fig. 2. Dependence of the Raman intensity ratio, I_D/I_G, as functions of target power and Ag/C ratio in films.

attributed to silver existing in carbon in the different forms when the contents of silver increase. The graphitization of the a-C:H matrix may not only affect the mechanical and electrical behavior but also lower down the surface energy of the films. The XRD patterns of the deposited films are shown in Fig. 3. The films deposited at target power above 100 W exhibit diffraction peaks of face-centered cubic silver crystal structure, and the intensity of peak increases with the contents of Ag. The film deposited at 100 W shows only the typical diffraction feature of the a-C:H film. This implies that a trace of silver could be completely solidified in the a-C:H phase. However, the presence of crystalline silver

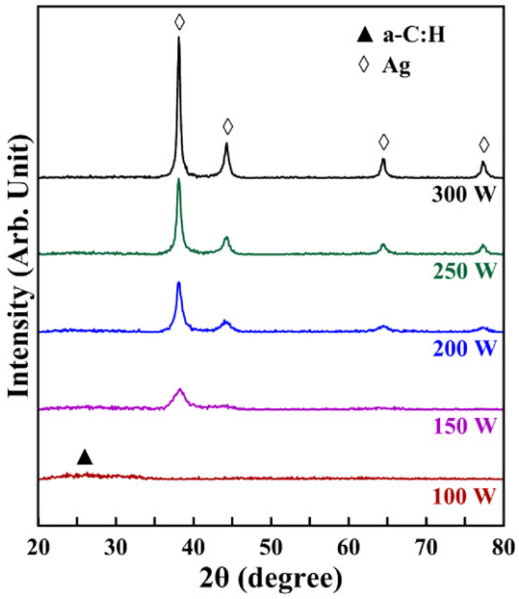

Fig. 3. XRD patterns of films deposited at different target powers.

phase in the films was observed when higher amounts of silver were doped, which reveals that the excess silver would segregate from the a-C:H matrix and cause a composite structure. These results concur with those proposed by Choi, who deposited Ag-incorporated a-C:H films utilizing ion beams [32]. The increase in intensity of silver XRD peak also reveals that both the grain size and the amount of segregated silver phase increase with the silver target power and silver content in the films.

The presence of secondary phase usually influences the surface morphology and properties of composite films. The surface morphologies of films deposited at different target powers are shown in Fig. 4, which also reveals the segregation of secondary phase. With increasing target power and silver content, the film surface gradually turns from flat into granular. This phenomenon is similar to those of the Ag-incorporated a-C:H films by other deposition process [32–34]. The granules on film surface could be the segregated silver phase as reported. The TEM observations also confirm these results of XRD patterns and surface morphologies. The films deposited at 100 W (Fig. 5a) show only a-C:H phase without segregation phase, as the same as that of the typical PECVD deposited a-C:H film. In contrast, spherical granules with a diameter of approximate 40 nm can be found in films deposited at higher target power (Fig. 5b and c). The amount of granules increases with the sputtering target power and silver content in film. The high resolution TEM images and selected-area diffraction patterns of granules (Fig. 6) demonstrate that these granules are silver clusters with a face-centered cubic structure. These granules show several crystal orientations with silver the inter-plane distance 2.36 Å, and the identified dot ring diffraction pattern also indicates that they are polycrystalline silver clusters. These evidences reveal that the surface granules in Fig. 4 are

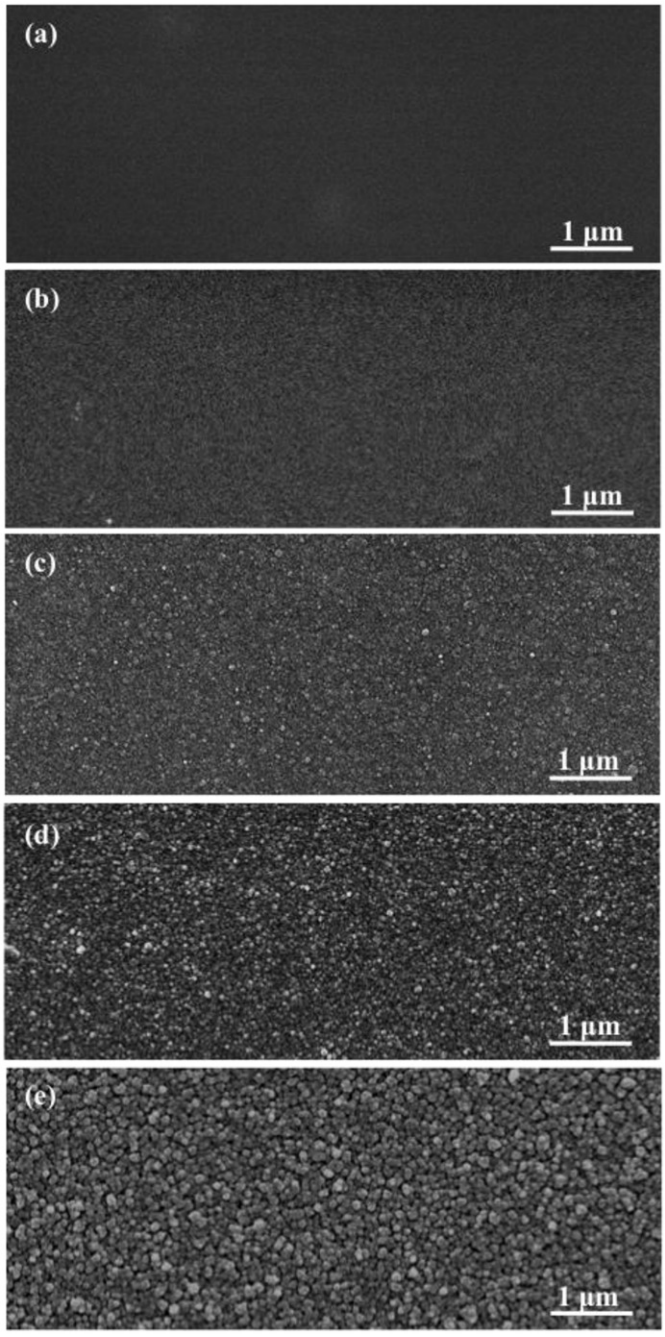

Fig. 4. SEM surface images of films deposited at different target powers (a) 100 W, (b) 150 W, (c) 200 W, (d) 250 W and (e) 300 W.

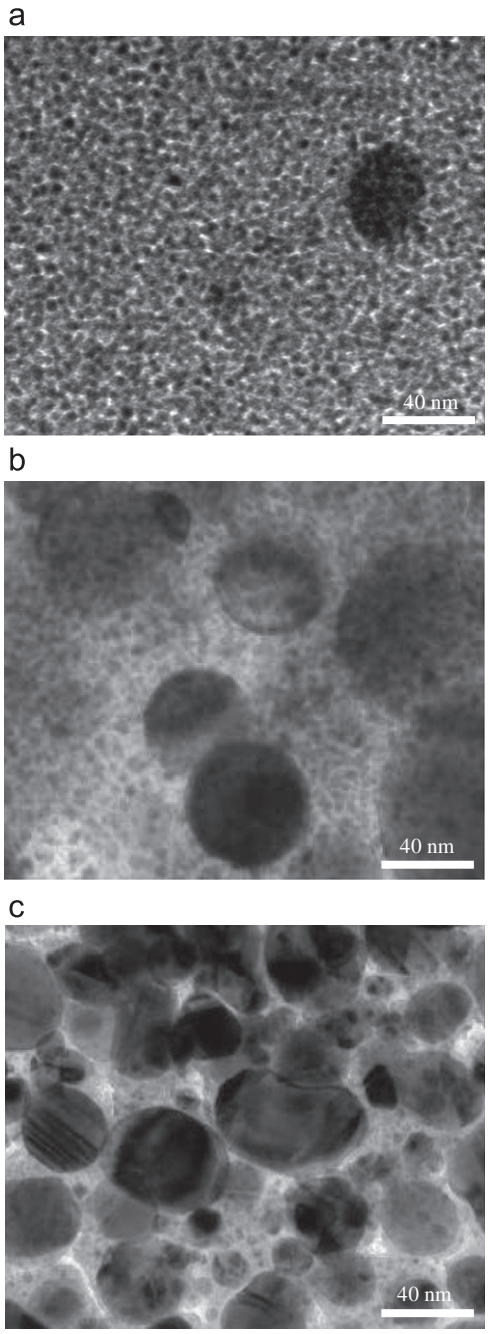

Fig. 5. TEM bright-field surface image of the Ag/a-C:H film deposited at the target power of (a) 100 W, (b) 200 W and (c) 300 W.

clusters of nanocrystals. This nanoparticle composite feature concurs with results of other deposition process of Ag-incorporated films [32–34]; the excess silver content segregates as secondary phase in a-C:H matrix due to the chemical inertness of silver and carbon elements. A (amorphous→amorphous-like→nanocrystalline structure) transition occurred during formation of Ag-incorporated a-C:H films. Previous study indicated that metal species contained in DLC film could result in a negative electrostatic surface [30]. In present study, compared to the a-C:H film, the nanocrystalline Ag-incorporated a-C:H film exists with more contact area and more negative electrostatic states, enhancing surface adsorption of calcium ions. The adsorption of positive ions such as calcium ions can mediate the adherence of the prealbumin, proteins albumin and immunoglobins from plasma. The adsorption of these proteins can improve the initial hemocompatibility and can decrease platelet activation, enhancing biocompatibility. Therefore, the Ag-incorporated a-C:H film is considered to possess biocompatibility.

Fig. 7 shows the surface roughness of films measured by AFM. The films with a higher Ag content and larger nanocluster size exhibit a higher surface roughness. When

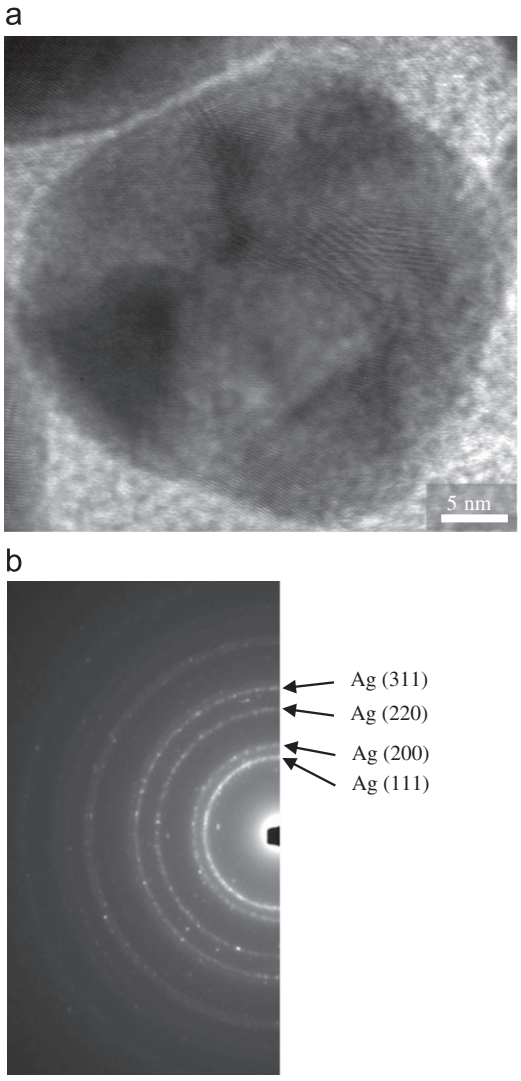

Fig. 6. (a) HR-TEM image of the silver cluster in the Ag/a-C:H film deposited at the target power of 300 W. (b)Diffraction pattern of an Ag cluster.

the target power is above 200 W, the films contain high excess silver composition, and the granular feature becomes visible on film surface (as shown in Fig. 4), and the surface roughness of the film simultaneously increases. Such change of roughness and silver clusters influence the optical, tribological and biomedical performances of these Ag/a-C:H composite films for future potential applications.

4. Conclusions

Bioceramic films were fabricated by reactive radio frequency magnetron sputtering using single silver target in an atmosphere of Ar/CH4 mixture. The films growth rate and content of silver in the diamond-like carbon matrix increased with the target power. In addition, a phase transformation, amorphous diamond-like carbon → nano-silver precipitation → nano-silver growth in the amorphous diamond-like carbon matrix was observed during sputtering. The presence of silver nanoclusters

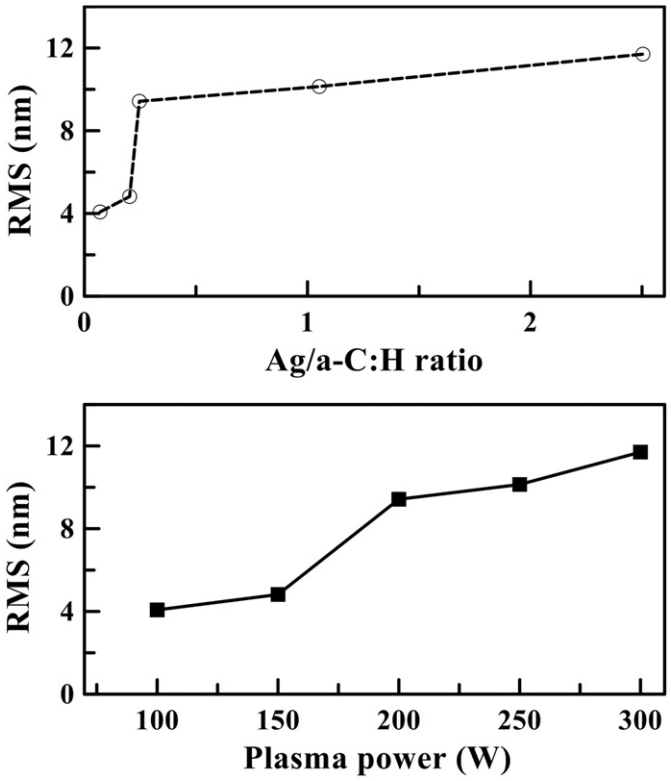

Fig. 7. Dependence of surface roughness as a function of (a) Ag/C ratio in film and (b) deposition target power.

significantly increased the surface roughness of the bioceramic films.

Acknowledgments

The authors would like to thank the Center of Excellence for Clinical Trial and Research in Neurology and Neurosurgery, Taipei Medical University-Wan Fang Hospital, for financially supporting this research under Contract no. DOH 101-TD-B-111-003, and by the Department of Health, Executive Yuan, Taiwan, for partly supporting by contract no. DOH101-TD-N-111-003.

References

[1] P.K. Bachmann, R. Messier, Emerging technology of diamond thin films, Chemical and Engineering News 67 (1989) 24–39.
[2] K.E. Spear, Growth of crystalline diamond from low pressure gases, Earth and Mineral Science 56 (1987) 53–59.
[3] K. Jia, Y.Q. Li, T.E. Fischer, B. Gallois, Tribology of diamond-like carbon sliding against itself, silicon nitride, Journal of Materials Research 10 (1995) 1403–1410.
[4] C. Jaoul, O. Jarry, P. Tristant, T. Merle-Mejean, M. Colas, C. Dublanche-Tixier, J.M. Jacquet, Raman analysis of DLC coated engine components with complex shape: understanding wear mechanisms, Thin Solid Films 518 (2009) 1475–1479.
[5] A. Grill, Diamond-like carbon coatings as biocompatible materials—an overview, Diamond Related Materials 12 (2003) 166–170.
[6] G. Dearnaley, J.H. Arps, Biomedical applications of diamond-like carbon (DLC) coatings: a review, Surface and Coatings Technology 200 (2005) 2518–2524.

[7] C. Nørgård, S.S. Eskildsen, A. Matthews, Engineering applications for diamond-like carbon, Surface and Coatings Technology 74–75 (1995) 358–361.
[8] S.J. Dowey, K.M. Read, K.S. Fancey, A. Matthews, The penetration into blind Holes of diamond-like carbon films produced by rf plasma assisted CVD, Surface and Coatings Technology 74–75 (1995) 710–716.
[9] X.M. He, W.Z. Li, H.D. Li, Ion beam assisted deposition of diamond-like carbon onto steel materials: preparation and advantages, Surface and Coatings Technology 84 (1996) 414–419.
[10] J. Deng, M. Braun, DLC multiplayer coatings for wear protection, Diamond Related Materials 4 (1995) 936–943.
[11] N.A. Sánchez, C. Rincón, G. Zambrano, H. Galindo, P. Prieto, Characterization of diamond-like carbon (DLC) thin films prepared by r.f. magnetron sputtering, Thin Solid Films 373 (2000) 247–250.
[12] D.Y. Wang, K.W. Weng, C.L. Chang, X.J. Guo, Tribological performance of metal doped diamond-like carbon films deposited by cathodic arc evaporation, Diamond Related Materials 9 (2000) 831–837.
[13] V.N. Inkin, G.G. Kirpilenko, A.A. Dementjev, K.I. Maslakov, A superhard diamond-like carbon film, Diamond Related Materials 9 (2000) 715–721.
[14] Akira Doi, Hiromu Kawai, Takashi Yoshioka, Shosaku Yamanaka, Vapor-deposited ceramic coating: status and prospects, Ceramic International 18 (1992) 223–229.
[15] K.A. Pischow, J. Koskinen, M. Adamik, P.B. Barna, Cross-sectional scanning force microscopy analysis of arc-discharge-deposited diamond-like carbon films, Ceramic International 22 (1996) 49–52.
[16] N. Mutsukuza, S. Tomita, Y. Mizum, The mechanical properties of hydrogenated hard carbon films, Thin Solid Films 214 (1992) 58–62.
[17] J. Robertson, Properties of diamond-like carbon, Surface and Coatings Technology 50 (1992) 185–203.
[18] A. Grill, Review of the tribology of diamond-like carbon, Wear 168 (1993) 143–153.
[19] A. Grill, V. Patel, Tribological properties of diamond-like carbon and related materials, Diamond Related Materials 2 (1993) 597–605.
[20] C. Strondl, N.M. Carvalho, J.T.M. De Hosson, G.J. van der Kolk, Investigation on the formation of tungsten carbide in tungsten-containing diamond like carbon coatings, Surface and Coatings Technology 162 (2003) 288–293.
[21] A.A. Voevodin, J.M. Schneider, C. Caperaa, P. Stevenson, A. Matthews, Characterisation of a saddle field source for deposition of diamond-like carbon films, Ceramic International 22 (1996) 1–5.
[22] W.Y. Wu, J.M. Ting, Growth and characteristics of metal-containing diamond-like carbon using a self-assembled process, Carbon 44 (2006) 1210–1217.
[23] Y.H. Chan, C.F. Huang, K.L. Ou, P.W. Peng, Mechanical properties and antibacterial activity of copper doped diamond-like carbon films, Surface and Coatings Technology 206 (2011) 1037–1040.
[24] S.C.H. Kwok, W. Zhang, G.J. Wan, D.R. McKenzie, M.M.M. Bilek, Paul K. Chu, Hemocompatibility and anti-bacterial properties of silver doped diamond-like carbon prepared by pulsed filtered cathodic vacuum arc deposition, Diamond Related Materials 16 (2007) 1353–1360.
[25] O. Garcia-Zarco, S.E. Rodil, M.A. Camacho-López, Deposition of amorphous carbon–silver composites, Thin Solid Films 518 (2009) 1493–1497.
[26] T.N. Kim, Q.L. Feng, J.O. Kim, J. Wu, H. Wang, G.C. Chen, F.Z. Cui, Antimicrobial effects of metal ions (Ag(+), Cu(2+), Zn(2+)) in hydroxyapatite, Journal of Materials Science—Materials in Medicine 9 (1998) 129–134.
[27] A.D. Russell, W.B. Hugo, Antimicrobial activity and action of silver, Progress in Medicinal Chemistry 31 (1994) 351–358.
[28] V. Alt, T. Bechert, P. Steinrücke, M. Wagener, P. Seidel, E. Dingeldein, E. Domann, R. Schnettler, An in vitro assessment of the antibacterial properties and cytotoxicity of nanoparticulate silver bone cement, Biomaterials 25 (2004) 4383–4391.
[29] X.B. Tian, Z.M. Wang, S.Q. Yang, Z.J. Luo, Ricky K.Y. Fu, Paul K. Chu, Antibacterial copper-containing titanium nitride films produced by dual magnetron sputtering, Surface and Coatings Technology 201 (2007) 8606–8609.
[30] H.C. Cheng, S.Y. Chiou, C.M. Liu, M.H. Lin, C.C. Chen, K.L. Ou, Effect of plasma energy on enhancing biocompatibility and hemocompatibility of diamond-like carbon film with various titanium concentrations, Journal of Alloys and Compounds 477 (2009) 931–935.
[31] W.C. Feng, C.H. Wang, H.C. Cheng, S.Y. Chiou, C.S. Chen, K.L. Ou, Enhancement of hemocompatibility on titanium implant with titanium-doped diamond-like carbon film evaluated by cellular reactions using bone marrow cell cultures in vitro, Journal of Vacuum Science and Technology B 27 (2009) 1559–1565.
[32] H.W. Choi, J.H. Choi, K.R. Lee, J.P. Ahn, K.H. Oh, Structure and mechanical properties of Ag-incorporated DLC films prepared by a hybrid ion beam deposition system, Thin Solid Films 516 (2007) 248–251.
[33] K. Baba, R. Hatada, S. Flege, W. Ensinger, Preparation and properties of Ag-containing diamond-like carbon films by magnetron plasma source ion implantation, Advances in Materials Science and Engineering (2012) 536853 Article ID.
[34] R. Paul, S. Dalui, A.K. Pal, Modulation of field emission properties of DLC films with the incorporation of nanocrystalline silver nanoparticles by CVD technique, Surface and Coatings Technology 204 (2010) 4025–4033.